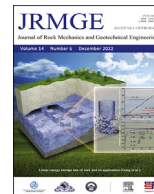




Contents lists available at ScienceDirect

Journal of Rock Mechanics and Geotechnical Engineering

journal homepage: www.jrmge.cn

Full Length Article

Theoretical verification of the rationality of strain energy storage index as rockburst criterion based on linear energy storage law

Fengqiang Gong^{a,b,c,d,*}, Song Luo^c, Quan Jiang^d, Lei Xu^c

^a Engineering Research Center of Safety and Protection of Explosion and Impact of Ministry of Education (ERCSPME), Southeast University, Nanjing, 211189, China

^b School of Civil Engineering, Southeast University, Nanjing, 211189, China

^c School of Resources and Safety Engineering, Central South University, Changsha, 410083, China

^d State Key Laboratory of Geomechanics and Geotechnical Engineering, Institute of Rock and Soil Mechanics, Chinese Academy of Sciences, Wuhan, 430071, China

ARTICLE INFO

Article history:

Received 8 July 2021

Received in revised form

12 September 2021

Accepted 2 December 2021

Available online 25 January 2022

Keywords:

Rockburst criterion

Strain energy storage index

Linear energy storage (LES) law

Peak-strength strain energy storage index

ABSTRACT

The rationality of using strain energy storage index (W_{et}) for evaluating rockburst proneness was theoretically verified based on linear energy storage (LES) law in this study. The LES law is defined as the linear relationship between the elastic strain energy stored inside the solid material and the input strain energy during loading. It is used to determine the elastic strain energy and dissipated strain energy of rock specimens at various loading/unloading stress levels. The results showed that the W_{et} value obtained from experiments was close to the corresponding theoretical one from the LES law. Furthermore, with an increase in the loading/unloading stress level, the ratio of elastic strain energy to dissipated strain energy converged to the peak-strength strain energy storage index (W_{et}^p). This index is stable and can better reflect the relative magnitudes of the stored energy and the dissipated energy of rocks at the whole pre-peak stage than the strain energy storage index. The peak-strength strain energy storage index can replace the conventional strain energy storage index as a new index for evaluating rockburst proneness.

© 2022 Institute of Rock and Soil Mechanics, Chinese Academy of Sciences. Production and hosting by Elsevier B.V. This is an open access article under the CC BY-NC-ND license (<http://creativecommons.org/licenses/by-nc-nd/4.0/>).

1. Introduction

Rockburst is the sudden release of accumulated elastic strain energy in highly stressed rocks and is a type of disaster frequently encountered in deep rock projects (Singh, 1988; He et al., 2010; Feng et al., 2012; Kaiser and Cai, 2012; Cai, 2016, 2019; Zhang et al., 2016; Makowski and Niedbalski, 2020). Numerous studies have shown that energy analysis is a practical approach for evaluating the outburst risk in rock engineering (Mitri et al., 1993, 1999). Rockburst proneness is typically regarded as a property that characterizes the outburst potential of rocks in terms of mechanical and energy parameters. Its determination could provide guidance and help control/prevent rockburst disasters in engineering practice (Tang et al., 2010; He et al., 2012a, b; Zhang et al., 2012; Li et al., 2017; Gong et al., 2020; Li, 2021; Xu et al., 2021). Under external

loadings, rocks could experience the stages of input, storage, and dissipation of strain energy, and the accumulated elastic strain energy plays a significant role in ejecting rock fragments during rock failure (Xie et al., 2009; Jiang et al., 2015; Gong et al., 2018a; Simser, 2019). For brittle rocks, the ratio of stored elastic strain energy to dissipated strain energy can reflect the performance of energy storage in rock under loading and during rockburst. Hence, it is essential to evaluate the burst proneness of rocks from energy storage and dissipation perspectives.

In the past few decades, different energy indices have been proposed for assessing the burst proneness of rocks (Kidybiński, 1981; Tjongkie, 1986; Singh, 1988; Tan, 1992; Wang and Park, 2001; Qiu et al., 2011; Gong et al., 2018b, 2019a, 2020). For example, through analyses of energy variations during rock deformation and breaking, Singh (1988) introduced the 'burst energy release index' to describe the energy released at the time of fracturing. Tan (1992) defined the elastic strain energy of rock at the state between ejection and non-ejection as the critical ejection energy. Deng et al. (2012) put forward the rockburst energy index to evaluate the rockburst proneness considering the stress-strain relationship of rock. Gong et al. (2018b, 2019a) discovered the linear energy storage (LES) law in uniaxial compressed rocks, based

* Corresponding author. Engineering Research Center of Safety and Protection of Explosion and Impact of Ministry of Education (ERCSPME), Southeast University, Nanjing, 211189, China.

E-mail address: fengqiangg@126.com (F. Gong).

Peer review under responsibility of Institute of Rock and Soil Mechanics, Chinese Academy of Sciences.

on which the peak-strength strain energy storage index and residual elastic energy index were introduced to the burst proneness assessment of rocks. Among these indices, the strain energy storage index (W_{et}) is the most widely used one. W_{et} was presented by Neyman et al. (1972) and Szczowka et al. (1973) when the energy index concept was introduced to classify coals according to their respective bursting liabilities. Several years later, Kidybiński (1981) introduced a method to calculate W_{et} with the single-cyclic loading-unloading uniaxial compression test. W_{et} was measured using the elastic strain energy and dissipated strain energy when the exerted stress was approximately 0.8–0.9 times the peak strength (σ_c) of the coal specimens. Since then, this energy index has been used by several researchers to analyze the burst proneness of rocks. It has also been applied to rockburst risk evaluation in rock mechanics and geotechnical engineering fields. Furthermore, W_{et} has been incorporated into the energy industry standard of China as a recommended index for assessing the rockburst risk in 2019 (NB/T 10143–2019, 2019), which signified the broad application of W_{et} . Although W_{et} has been generally accepted and widely used, the rationality of the usage of W_{et} has not been proven. In other words, the principle of the W_{et} calculation lacks theoretical verification.

In this study, based on the LES law (Gong et al., 2018b; 2019b), the rationality of W_{et} used for evaluating rockburst proneness was theoretically derived and verified. The experimental data on several typical rocks with different degrees of burst proneness (e.g. high, moderate, slight, and no burst proneness) were employed for verification. Furthermore, the peak-strength strain energy storage index (W_{et}^p , the ratio of elastic strain energy to dissipated strain energy at the peak strength of rock (Gong et al., 2019a)) was included for comparison. Based on the theoretical verification, W_{et}^p was recommended to replace the conventional W_{et} in assessing rockburst proneness.

2. Brief description of W_{et}

Neyman et al. (1972) and Szczowka et al. (1973) proposed an energy index to evaluate the burst proneness of coal. This index was subsequently adopted by Kidybiński (1981) in deriving the strain energy storage index (W_{et}) as follows:

$$W_{et} = \frac{U_e^{0.8}}{U_d^{0.8}} \quad (1)$$

where $U_e^{0.8}$ and $U_d^{0.8}$ are the elastic strain energy and dissipated strain energy under the uniaxial compression of rock when the exerted stress (σ) reaches 80%–90% (i.e. $i = 0.8–0.9$, where i is the unloading stress level) of the peak strength σ_c (Fig. 1). The initial grading of W_{et} is listed in Table 1.

In 1988, W_{et} was adopted as a rockburst proneness index (Singh, 1988). As W_{et} has a simple mathematical form and is easy to obtain, it has been frequently used by many scholars. The citation frequencies of W_{et} in the literature from 1984 to 2020 are shown in Fig. 2. The number of citations has increased sharply since 2004, reaching 47 in 2020 (Fig. 2), indicating that the rockburst proneness criterion, particularly W_{et} , has gained increasing attention. Furthermore, W_{et} has been widely used to evaluate rockburst proneness in different disciplines, such as mining engineering, geology, civil engineering, architecture, and water conservancy engineering.

In 2019, energy industry standard of China (NB/T 10143–2019, 2019) adopted W_{et} as an evaluation index of the rockburst intensity grade when in situ stress and related information was lacking or unclear. The grading standard of W_{et} for rock was also

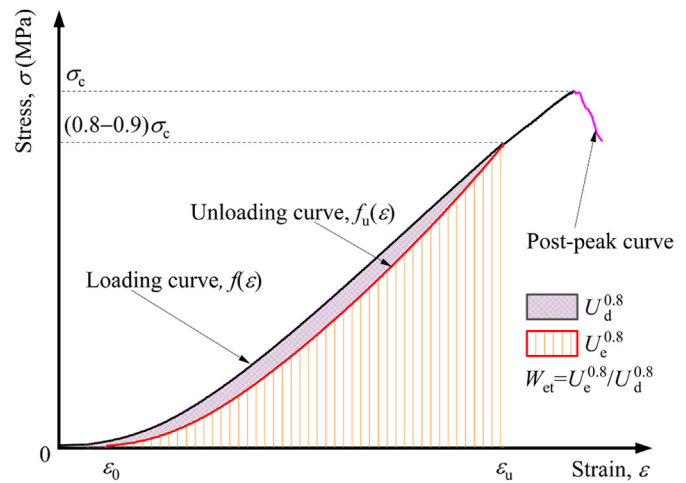


Fig. 1. Illustration of parameters used to calculate W_{et} .

Table 1
The initial grading of W_{et} .

Range of W_{et}	Grading
$W_{et} \geq 5.0$	High burst proneness
$2.0 \leq W_{et} < 4.99$	Low burst proneness
$W_{et} < 2.0$	No burst proneness

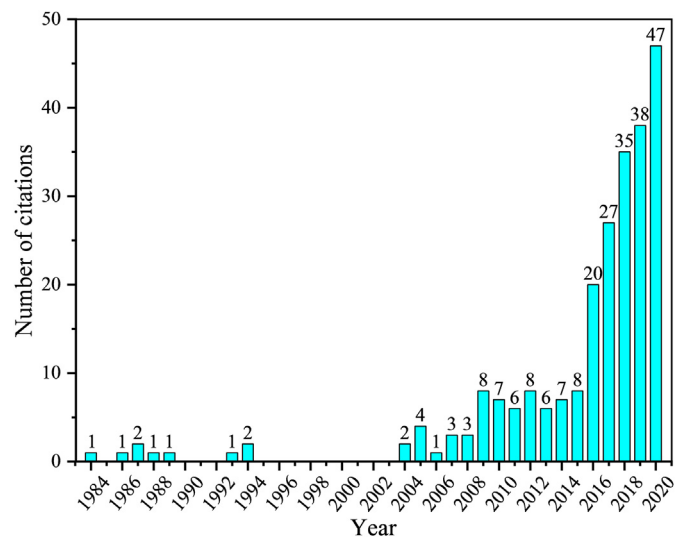


Fig. 2. Citation frequencies of W_{et} in the literature.

provided. The burst proneness was divided into four levels and measured based on loading–unloading tests with the unloading stress level (i) of 0.7–0.8. The updated grading of W_{et} is shown in Table 2.

Table 2
The updated grading of W_{et} .

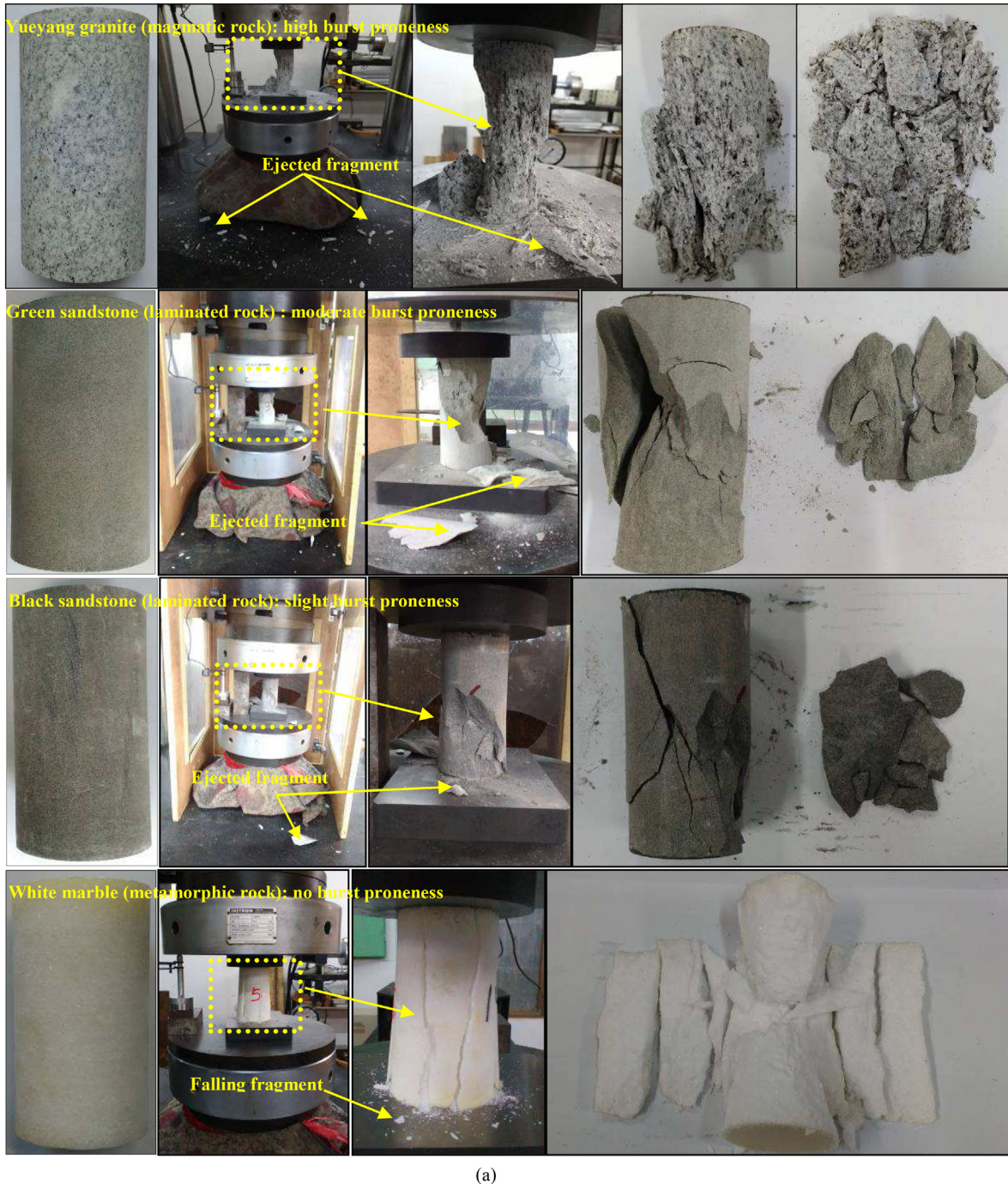
Range of W_{et}	Grading
$W_{et} \geq 5.0$	High or extremely high burst proneness
$3.5 \leq W_{et} < 5.0$	Moderate burst proneness
$2.0 \leq W_{et} < 3.5$	Slight/low burst proneness
$W_{et} < 2.0$	No burst proneness

As mentioned above, W_{et} has been widely used in rock engineering, indicating that this index has been generally accepted to be useful in assessing rockburst proneness. However, deficiency of W_{et} still exists. By comparing the two aforementioned determining methods of W_{et} , it can be found that the difference exists in the corresponding range of i when calculating W_{et} with ranges of 0.8–0.9 and 0.7–0.8 in the first and second methods, respectively. These two ranges have an overlapped value of 0.8 (Kidybiński, 1981; NB/T 10143–2019, 2019). The precise determining of the range of i leads to a question: Why is the value of i approximating 0.8 used for calculating W_{et} ? Thus far, no relevant proof has been provided. Furthermore, there has been no basis for determining the proper

interval of i at which the elastic strain energy and dissipated strain energy can be considered reliable for computing W_{et} . This problem has not been solved from a scientific perspective, and no theoretical verification of its rationality has been established. Therefore, we aimed to demonstrate the basis of establishing W_{et} using the LES law of rock.

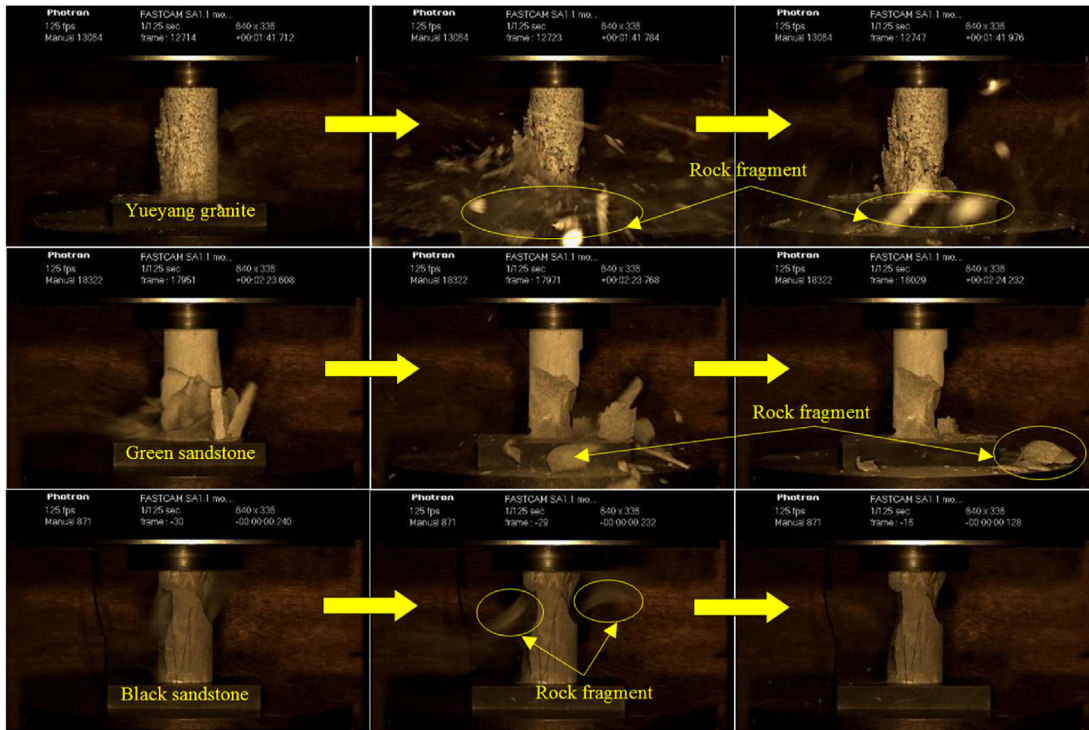
3. LES and linear energy dissipation (LED) laws of rock

From the energy point of view, the deformation of or damage to rocks occur because of the combined effects of energy input, accumulation, dissipation, and release. For a stressed rock element, the



(a)

Fig. 3. Typical rock specimens used for deriving the LES and LED laws: (a) Specimens before and after testing, and (b) Bursting scenarios of specimens (Gong et al., 2018b).



(b)

Fig. 3. (continued).

input strain energy U_0 includes the elastic strain energy U_e and dissipated strain energy U_d . Their correlation and calculation formulae can be expressed as follows (Kidybiński, 1981; Xie et al., 2005):

$$\left. \begin{aligned} U_0 &= U_e + U_d \\ U_e &= \int_{\epsilon_0}^{\epsilon_u} f_u(\epsilon) d\epsilon \\ U_d &= \int_0^{\epsilon_u} f(\epsilon) d\epsilon - \int_{\epsilon_0}^{\epsilon_u} f_u(\epsilon) d\epsilon \end{aligned} \right\} \quad (2)$$

where ϵ_0 denotes the permanent strain after unloading; ϵ_u refers to the strain corresponding to the unloading stress; and $f(\epsilon)$ and $f_u(\epsilon)$ are the functions describing the loading and unloading curves, respectively (Fig. 1).

Based on the energy principle expressed in Eq. (2), the LES and LED laws of rocks or coals under uniaxial compression were developed (Gong et al., 2018b; 2019a; b, 2021). In this work, the LES relationships of four representative rocks with different degrees of burst proneness were used for verifying the applicability of W_{et} in rockburst analysis. Fig. 3 shows the four representative rocks, which cover three major types (i.e. magmatic, metamorphic, and laminated rocks) with distinct degrees of burst proneness (see the broken and bursting scenarios of the rock specimens shown in Fig. 3). Fig. 4 shows the LES and LED laws of rocks with high coefficient of determination, R^2 . The LES law is interpreted as a linear correlation between the elastic strain energy and input strain energy. Similarly, the LED law shows a linear correlation between the dissipated strain energy and input strain energy (Gong et al., 2018b). The elastic, dissipated, and input strain energies (mJ/mm^3) were used in the LES and LED

laws. They can be directly calculated by integrating the associated segments in the resultant stress-strain curves (e.g. elastic strain energy can be determined by integrating the unloading curve), as illustrated by the shaded areas in Fig. 1. Fig. 4 shows their correlative LES and LED laws. In essence, the LES and LED laws should predict elastic and dissipated strain energies to be zero at the initial state when the input strain energy is zero. Therefore, the ideal theoretical equations for the LES and LED laws are written as

$$\left. \begin{aligned} U_e^i &= aU_0^i \\ U_d^i &= (1 - a)U_0^i \end{aligned} \right\} \quad (3)$$

where U_0^i , U_e^i , and U_d^i are the input, elastic, and dissipated strain energies at the unloading stress level i ($i = 0-1$), respectively. The variable ‘ a ’ represents the energy storage coefficient under uniaxial compression (Gong et al., 2018b; 2019a).

In the analysis, a constant term, b , was generated in the LES and LED laws when fitting the experimental data of rock specimens. The generation of b is attributed to the discreteness and anisotropy of specimens, and it appears to be smaller than a (Gong et al., 2018b). Therefore, the general theoretical formulae of the LES and LED laws can be expressed as

$$\left. \begin{aligned} U_e^i &= aU_0^i + b \\ U_d^i &= (1 - a)U_0^i - b \end{aligned} \right\} \quad (4)$$

Additionally, we also verified the LES and LED laws using the data under multiple cyclic loading-unloading uniaxial compression tests from the stress-strain curves published by other researchers

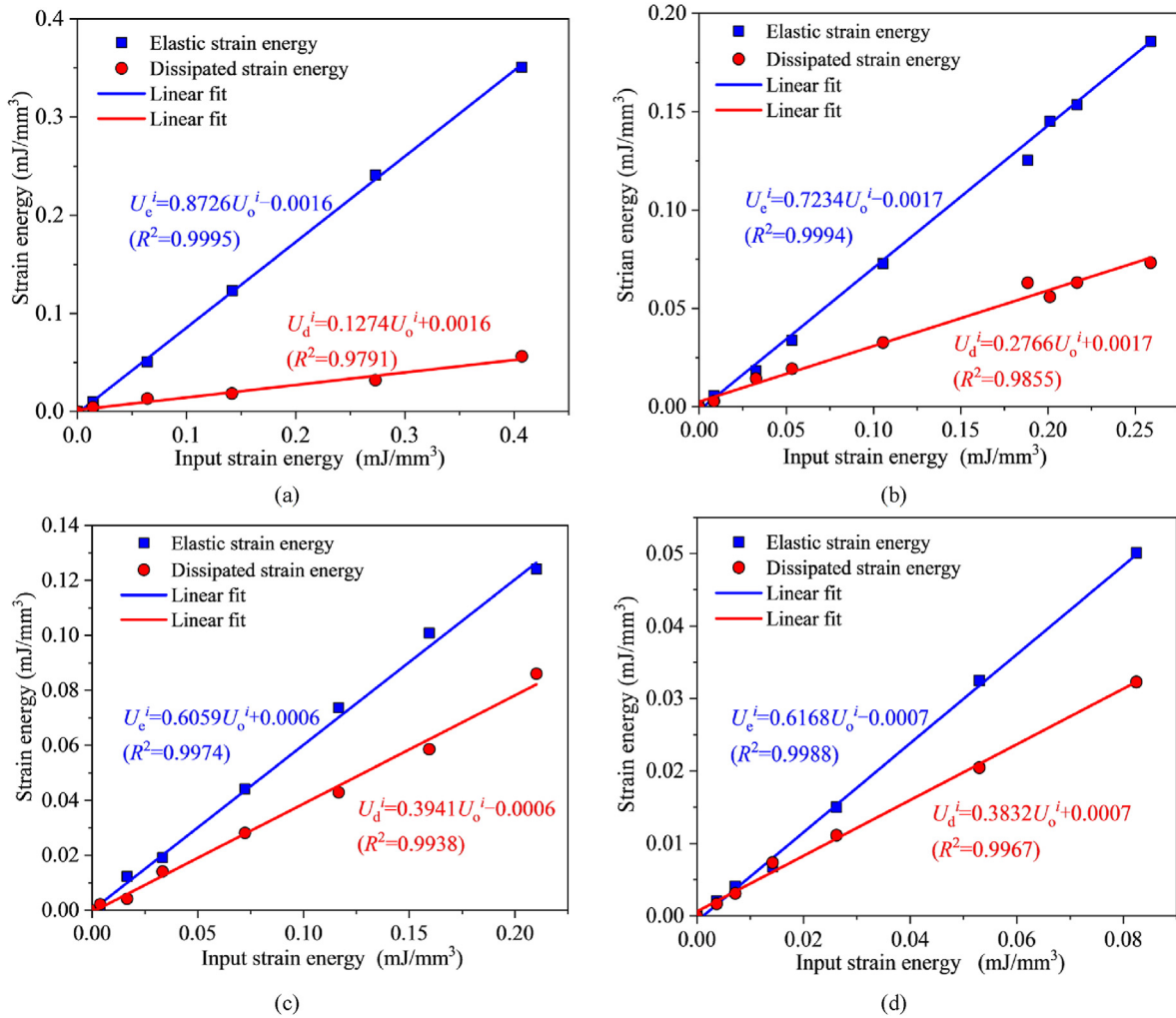


Fig. 4. Linear energy correlations for four representative rocks (Gong et al., 2018b): (a) Yueyang granite, (b) Green sandstone, (c) Black sandstone, and (d) White marble.

(Meng et al., 2016; Wang et al., 2018). They also match well with relationships of LES and LED laws (Fig. 5).

Based on the above analysis, the LES and LED laws are universal for different rocks. This can be supported by three observations:

- (1) The LES and LED laws are independent of the type of rocks. The evaluated rocks were of three major types: magmatic, metamorphic, and laminated rocks. The evolutions of elastic and dissipated strain energies against the input strain energy of all types can be characterized using the LES and LED laws.
- (2) They are independent of the mechanical properties of rocks. Although the mechanical parameters (e.g. compressive strength and modulus of elasticity) and elastic brittleness (or plasticity) of rocks vary significantly, the LES and LED laws can still be valid.
- (3) The existence of LES and LED laws was also found to be independent of the rock failure patterns under one-dimensional or two-dimensional loading conditions (Luo and Gong, 2020a, b; Su et al., 2021).

Therefore, we can use the LES and LED laws to verify the rationality of W_{et} , as discussed in the following section.

4. Analysis of W_{et}

4.1. Concept of strain energy storage ratio

The strain energy storage ratios include the ratio (W_{et}^i) of experimental elastic strain energy to dissipated strain energy, the ideal theoretical strain energy storage ratio (W_{I-et}^i), and the general theoretical strain energy storage ratio (W_{G-et}^i). They reflect the variation in the ratio of elastic strain energy to dissipated strain energy at different unloading stress levels. For a specific rock material, W_{I-et}^i can be determined using Eq. (3) as

$$W_{I-et}^i = \frac{U_e^i}{U_d^i} = \frac{aU_o^i}{(1-a)U_o^i} \quad (5)$$

Similarly, W_{G-et}^i can be obtained using Eq. (4) as

$$W_{G-et}^i = \frac{U_e^i}{U_d^i} = \frac{aU_o^i + b}{(1-a)U_o^i - b} \quad (6)$$

By applying the general theoretical formulae of the LES and LED laws, the elastic and dissipated strain energies at the peak strength

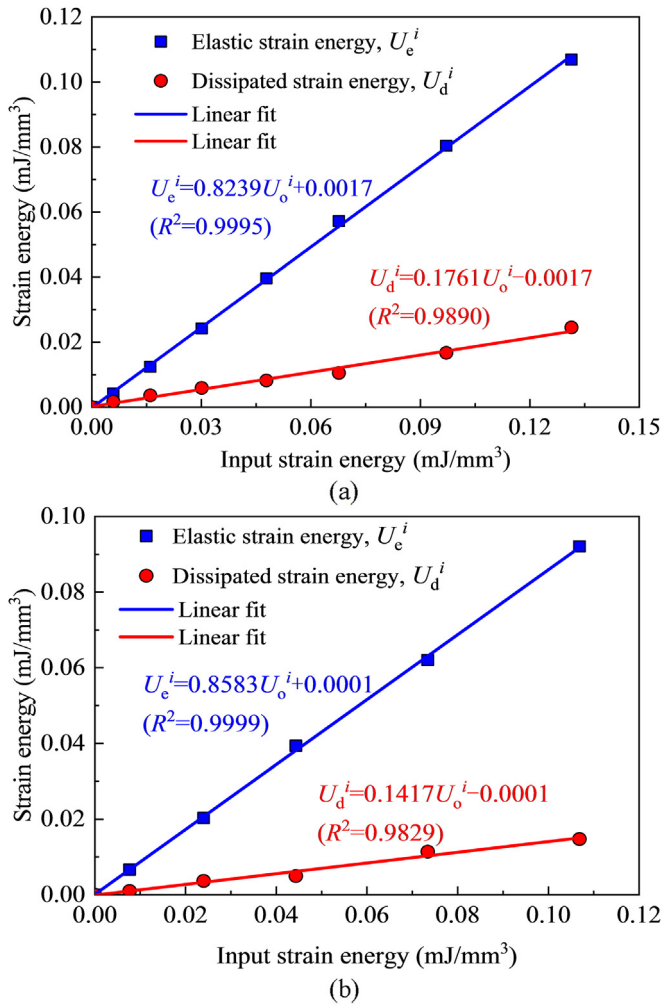


Fig. 5. Verifications of LES and LED laws for (a) red sandstone (Meng et al., 2016) and (b) granite (Wang et al., 2018).

can be obtained accurately. In addition, the peak-strength strain energy storage index (W_{et}^p) is defined based on Gong et al. (2019a) as

$$W_{et}^p = \frac{U_e^p}{U_d^p} \tag{7}$$

where U_e^p and U_d^p are the elastic and dissipated strain energies at the peak strength of rock, respectively. U_e^p and U_d^p are obtained using the general theoretical equations of the LES and LED laws. The related grading of W_{et}^p is listed in Table 3.

4.2. Variation of W_{et}

From the results obtained in the single-cyclic loading-unloading uniaxial compression experiments, the dependence of the input strain energy on i has been observed. Based on this relationship, using Eqs. (5) and (6), the variations in W_{1-et}^i and W_{G-et}^i with i can be plotted, as shown in Fig. 6. For comparisons, the values of W_{et} , W_{et}^i , and \bar{W}_{et}^p (\bar{W}_{et}^p is the average of W_{et}^p value of the tested specimens with the same rock lithology) are also included in Fig. 6.

Table 3
The related grading of W_{et}^p .

Range of W_{et}^p	Grading
$W_{et}^p > 5.0$	High burst proneness
$2.0 \leq W_{et}^p \leq 5.0$	Low burst proneness
$W_{et}^p < 2.0$	No burst proneness

When i was small, W_{et}^i (directly calculated using the experimental data) exhibited a significant degree of discreteness, and no regular pattern between W_{et}^i and i was observed (Fig. 6). As i increased, a clear relationship between W_{et}^i and i emerged, i.e. W_{et}^i converged to \bar{W}_{et}^p . In contrast, a noticeable correlation between W_{G-et}^i and i can always be observed. When i was relatively small, W_{G-et}^i was more affected by the constant b (see Eq. (6)), while it was less affected by b when i was comparatively large ($i > 0.4$). For extreme large value of i , the influence of b was weakened and W_{G-et}^i gradually converged to \bar{W}_{et}^p . However, W_{1-et}^i was a constant independent of i , as it was deduced from the ideal theoretical formula in which the constant b was not included (see Eq. (5)). The above difference occurred when i was small, when the absolute magnitudes of both elastic and dissipated strain energies were low. In this case, small changes in the amount of these two strain energy parameters could significantly influence their ratios, and thus, W_{et}^i appeared to have no consistent correlation with i . The main reason was that W_{et}^i was sensitive at a low value of i . As i increased gradually, the absolute magnitude of the measured elastic and dissipated strain energies increased, and the sensitivity of W_{et}^i to i decreased. Thus, the convergence occurred gradually. For rockburst problems, attention was generally focused on the obtained value of W_{et}^i , as i was larger than 0.8. This signifies that the parameter W_{et}^i is stable and is a desired parameter for evaluating rockburst proneness.

Furthermore, W_{G-et}^i exhibited a significant convergence trend as i increased, and its value converged to \bar{W}_{et}^p , which was close to W_{1-et}^i , indicating that \bar{W}_{et}^p was relatively stable and the most desired result (in Fig. 7, the relative deviation and absolute difference between \bar{W}_{et}^p and W_{1-et}^i are minimal). In addition, it was found that when i was approximately 0.8, W_{et} was close to the corresponding value of W_{G-et}^i (Fig. 8) and the associated \bar{W}_{et}^p . This finding is our major focus in this study. Therefore, the desired value of W_{et} can be deduced more precisely using the general theoretical formulae, and the LES and LED laws provide theoretical support for the rational determination of W_{et} .

5. Discussion

5.1. Stability of W_{et}^p with respect to input strain energy

Even for the same rock material under uniaxial compression, the input strain energy required for rock specimens to reach their peak strengths differed because of the variation of rock strength. Therefore, we analyzed the variation of strain energy storage ratio with input strain energy to examine the applicability of W_{et} in rockburst analysis (Fig. 9). In addition to the experimental data of the four rocks above, those of the other four rocks (fine granite, yellow granite, yellow sandstone, and marble (Fig. 9e–h)) are also included for further examination (Gong et al., 2018b). Similar to the previous analysis in Section 4.2, W_{G-et}^i also converged to W_{et}^p over a wide range of input strain energy (Fig. 9), showing a similar variation of W_{G-et}^i with i . This is because the constant b influences the calculation of W_{G-et}^i . When the input strain energy was relatively small, W_{G-et}^i was significantly influenced by b . Only when the input

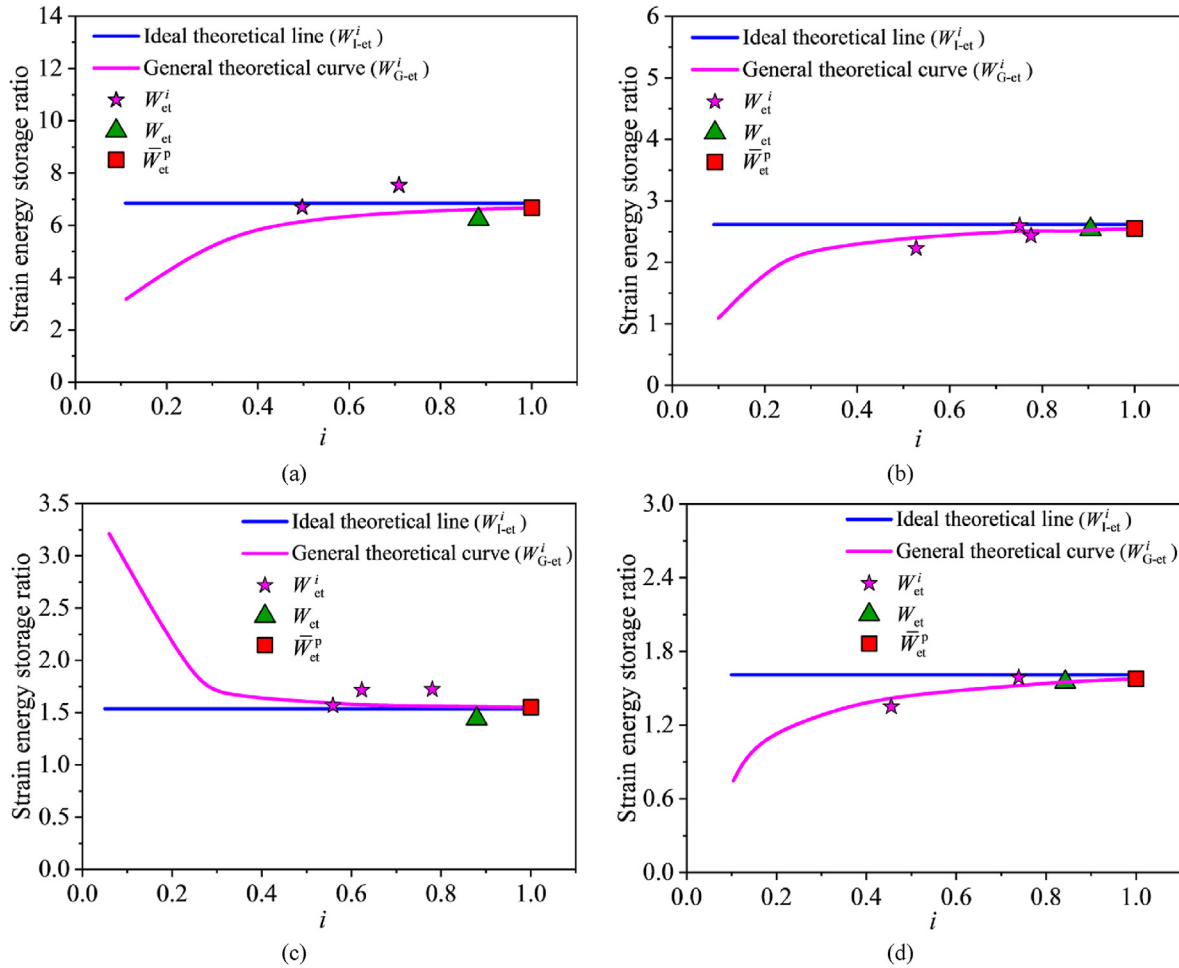


Fig. 6. Variations in W_{1-et}^i , W_{G-et}^i , and W_{et}^i with i : (a) Yueyang granite, (b) Green sandstone, (c) Black sandstone, and (d) White marble.

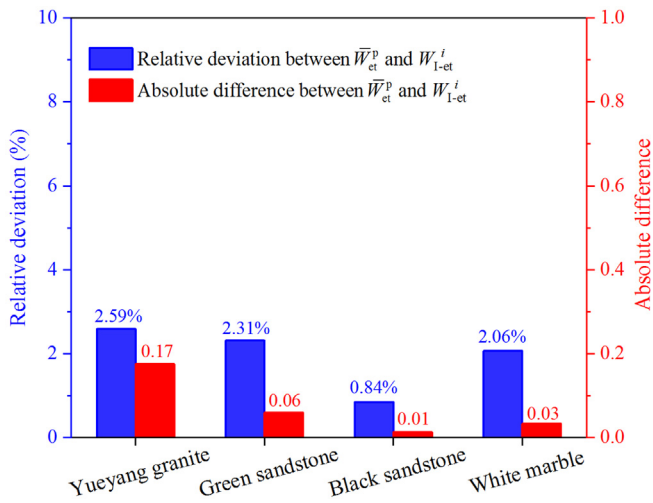


Fig. 7. Relative deviation and absolute difference between \bar{W}_{et}^p and W_{1-et}^i .

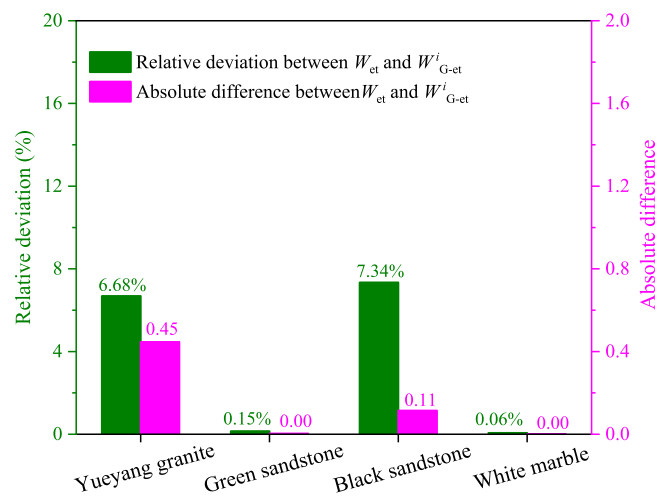


Fig. 8. Relative deviation and absolute difference between W_{et} and W_{G-et}^i .

strain energy was relatively large, W_{G-et}^i was less affected by b . As the input strain energy increased, the influence of b on W_{G-et}^i became increasingly small. Since the calculation of W_{1-et}^i did not

involve the constant b , it was a constant and was independent of the magnitude of input strain energy. In addition, as the input strain energy increased, W_{et}^p approached W_{1-et}^i . The coefficients of variation (CoV) for the W_{et}^p data for six specimens prepared from the

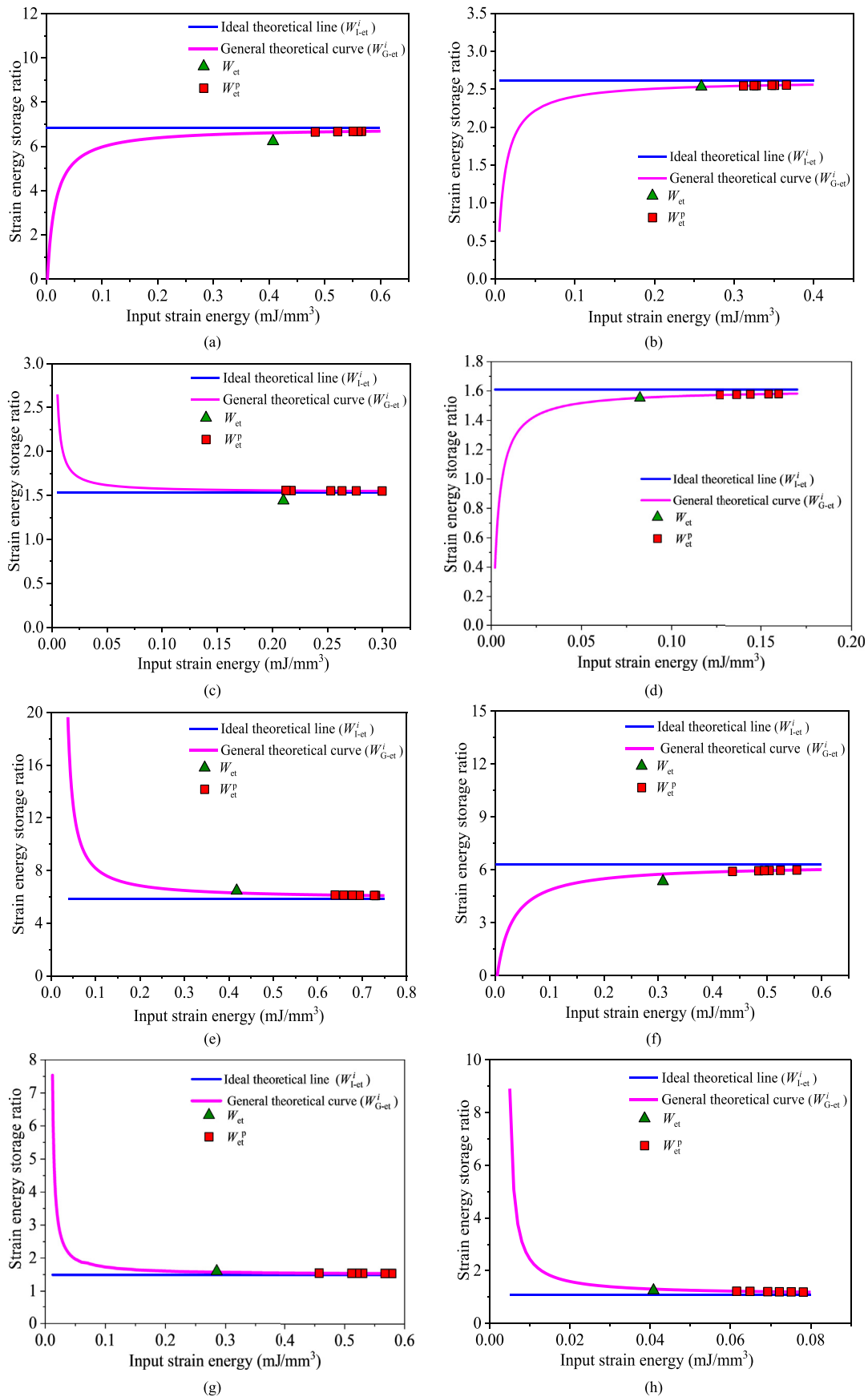


Fig. 9. Variations in strain energy storage ratio with input strain energy: (a) Yueyang granite, (b) Green sandstone, (c) Black sandstone, (d) White marble, (e) Fine granite, (f) Yellow granite, (g) Yellow sandstone, and (h) Marble.

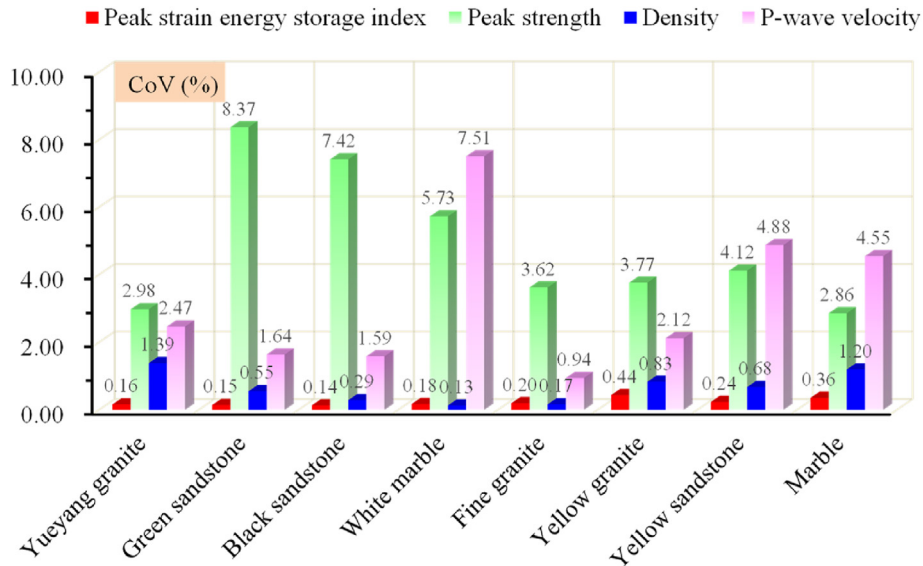


Fig. 10. CoV values of peak-strength strain energy storage index W_{et}^p , peak strength, density, and P-wave velocity of eight rocks.

same rock type are shown in Fig. 10. Compared with the CoV values of peak strength, density, and P-wave velocity, the CoV of W_{et}^p data were much smaller, suggesting that the W_{et}^p data has little variation, despite the change in input energy at rock failure. In other words, W_{et}^p was stable and suitable for characterizing the energy storage capacity of the rock. These observations on convergence for the input strain energy further demonstrates that W_{et}^p is better than W_{et} when estimating the burst proneness of rocks. Based on the analyses, W_{et}^p is a preferred parameter in practice, considering that rocks may exhibit heterogeneous behavior. In addition, W_{et}^p reflects the relative magnitude of the stored energy and the dissipated energy of rocks at the whole pre-peak loading stage, which can replace W_{et} as a new index for evaluating rockburst proneness of rock.

5.2. Deficiency of W_{et}^p

Although W_{et}^p is relatively stable and shows apparent superiority to W_{et} , it still has some disadvantages. For example, according to the gradings of W_{et} and W_{et}^p , the Yueyang granite, green sandstone, black sandstone, and white marble are subject to high, low, no, and no rock burst proneness, respectively. The assessments of green sandstone and black sandstone differed from their actual rock burst proneness (Fig. 3). This is because W_{et}^p only reflects the ratio of elastic strain energy to dissipated strain energy before the peak strength is reached, and it fails to quantify the energy transfer state from the peak strength to the post-peak bearing of rock specimens. Expressed in a ratio, it only characterizes a relative magnitude of the elastic strain energy to the dissipated strain energy, but cannot directly reflect an absolute energy state to describe rockburst potential. Hence, this index can only indicate the capacity of relative energy storage to energy consumption, and the absolute kinetic energy cannot be characterized when the rockburst occurs.

6. Conclusions

Based on the LES law in the uniaxial compression of rock, the rationality of determining the strain energy storage index (W_{et}) was verified theoretically in this study. It was observed that W_{et} consistently correlated with the corresponding W_{G-et}^i . Furthermore, W_{G-et}^i converged to the peak-strength strain energy storage

index (W_{et}^p) as the unloading stress level or input strain energy increased, and W_{et}^p more precisely approximated to the corresponding W_{G-et}^i than W_{et} . These findings demonstrate that W_{et}^p outperforms the conventional W_{et} , and thus W_{et}^p can be satisfactorily used as a substitute index of W_{et} for evaluating rockburst proneness of rock.

Declaration of competing interest

The authors declare that they have no known competing financial interests or personal relationships that could have appeared to influence the work reported in this paper.

Acknowledgments

This work was supported by the National Natural Science Foundation of China (Grant Nos. 42077244 and 41877272), and the Fundamental Research Funds for the Central Universities (Grant No. 22242022k30054).

List of symbols

a	Compression energy storage coefficient
b	Constant term
$f(\epsilon)$	Function describing the loading curve
$f_u(\epsilon)$	Function describing the unloading curve
i	Unloading stress level
σ	Exerted stress
σ_c	Peak strength
ϵ_0	Permanent strain after unloading
ϵ_u	Strain corresponding to the unloading stress level
R^2	Coefficient of determination
U_d	Dissipated strain energy
$U_d^{0.8}$	Dissipated strain energy under rock uniaxial compression when the exerted stress (σ) reaches $(0.8-0.9)\sigma_c$
U_d^i	Dissipated strain energy at unloading stress level of i
U_d^p	Dissipated strain energy at rock peak strength
U_e	Elastic strain energy
$U_e^{0.8}$	Elastic strain energy under rock uniaxial compression when the exerted stress (σ) reaches $(0.8-0.9)\sigma_c$
U_e^i	Elastic strain energy at unloading stress level of i

U_e^p	Elastic strain energy at rock peak strength
U_o	Input strain energy
U_o^i	Input strain energy at unloading stress levels of i
W_{et}	Strain energy storage index
W_{et}^i	Experimental elastic strain energy to dissipated strain energy ratio
W_{et}^p	Peak-strength strain energy storage index
\overline{W}_{et}^p	Average of W_{et}^p
W_{G-et}^i	General theoretical strain energy storage ratio
W_{I-et}^i	Ideal theoretical strain storage energy ratio

References

- Cai, M.F., 2016. Prediction and prevention of rockburst in metal mines—a case study of sanshandao gold mine. *J. Rock Mech. Geotech. Eng.* 8 (2), 204–211.
- Cai, M., 2019. Rock support in strainburst-prone ground. *Int. J. Min. Sci. Technol.* 29 (4), 8–13.
- Deng, L., Wu, J., Lu, Y., 2012. Study on rockburst energy index method based on the rock stress-strain curve. *Railway Standard Design* (7), 108–111 (in Chinese).
- Feng, X.T., Chen, B.R., Li, S.J., Zhang, C.Q., Xiao, Y.X., Feng, G.L., Zhou, H., Qiu, S.L., Zhao, Z.N., Yu, Y., Chen, D.F., Ming, H.J., 2012. Studies on the evolution process of rockbursts in deep tunnels. *J. Rock Mech. Geotech. Eng.* 4 (4), 289–295.
- Gong, F.Q., Luo, Y., Li, X.B., Si, X.F., Tao, M., 2018a. Experimental simulation investigation on rockburst induced by spalling failure in deep circular tunnels. *Tunn. Undergr. Space Technol.* 81, 413–427.
- Gong, F.Q., Yan, J.Y., Li, X.B., 2018b. A new criterion of rockburst proneness based on the linear energy storage law and the residual elastic energy index. *Chin. J. Rock Mech. Eng.* 37 (9), 1993–2014 (in Chinese).
- Gong, F.Q., Yan, J.Y., Li, X.B., Luo, S., 2019a. A peak-strength strain energy storage index for rock burst proneness of rock materials. *Int. J. Rock Mech. Min. Sci.* 117, 76–89.
- Gong, F.Q., Yan, J.Y., Luo, S., Li, X.B., 2019b. Investigation on the linear energy storage and dissipation laws of rock materials under uniaxial compression. *Rock Mech. Rock Eng.* 52 (11), 4237–4255.
- Gong, F.Q., Wang, Y.L., Luo, S., 2020. Rockburst proneness criteria for rock materials: review and new insights. *J. Cent. South Univ.* 27 (10), 2793–2821.
- Gong, F.Q., Wang, Y.L., Wang, Z.G., Pan, J.F., Luo, S., 2021. A new criterion of coal burst proneness based on the residual elastic energy index. *Int. J. Min. Sci. Technol.* 31, 553–563.
- He, M.C., Miao, J.L., Feng, J.L., 2010. Rock burst process of limestone and its acoustic emission characteristics under true-triaxial unloading conditions. *Int. J. Rock Mech. Min. Sci.* 47, 286–298.
- He, M.C., Jia, X.N., Coli, M., Livi, E., Sousa, L., 2012a. Experimental study of rockbursts in underground quarrying of Carrara marble. *Int. J. Rock Mech. Min. Sci.* 52 (1), 1–8.
- He, M.C., Xia, H.M., Jia, X.N., Gong, W.L., Zhao, F., Liang, K.Y., 2012b. Studies on classification, criteria, and control of rockbursts. *J. Rock Mech. Geotech. Eng.* 4 (2), 97–114.
- Jiang, Q., Su, G.S., Feng, X.T., Cui, J., Pan, P.Z., Jiang, J.Q., 2015. Observation of rock fragment ejection in post-failure response. *Int. J. Rock Mech. Min. Sci.* 74, 30–37.
- Kaiser, P.K., Cai, M., 2012. Design of rock support system under rockburst condition. *J. Rock Mech. Geotech. Eng.* 4 (3), 215–227.
- Kidybiński, A., 1981. Bursting liability indices of coal. *Int. J. Rock Mech. Min. Sci. Geomech. Abstr.* 18 (4), 295–304.
- Li, X.B., Gong, F.Q., Tao, M., Dong, L.J., Du, K., Ma, C.D., Zhou, Z.L., Yin, T.B., 2017. Failure mechanism and coupled static-dynamic loading theory in deep hard rock mining: a review. *J. Rock Mech. Geotech. Eng.* 9 (4), 767–782.
- Li, C.C., 2021. Principles and methods of rock support for rockburst control. *J. Rock Mech. Geotech. Eng.* 13 (1), 46–59.
- Luo, S., Gong, F.Q., 2020a. Linear energy storage and dissipation laws of rocks under preset angle shear conditions. *Rock Mech. Rock Eng.* 53 (7), 3303–3323.
- Luo, S., Gong, F.Q., 2020b. Linear energy storage and dissipation laws during rock fracture under three-point flexural loading. *Eng. Fract. Mech.* 234, 107102.
- Makowski, P., Niedbalski, Z., 2020. A comprehensive geomechanical method for the assessment of rockburst hazards in underground mining. *Int. J. Min. Sci. Technol.* 30 (3), 345–355.
- Meng, Q.B., Zhang, M.W., Han, L.J., Pu, H., Nie, T.Y., 2016. Effects of acoustic emission and energy evolution of rock specimens under the uniaxial cyclic loading and unloading compression. *Rock Mech. Rock Eng.* 49 (10), 1–14.
- Mitri, H.S., Hassan, F.P., Kebbe, R., 1993. A Strain Energy Approach for the Prediction of Rockburst Potential in Underground Hard Rock Mines. *Proceedings of the 1st*

- Canadian Symposium on Numerical Modelling Applications in Mining and Geomechanics. McGill University, Montreal, Canada, pp. 228–239.
- Mitri, H.S., Tang, B., Simon, R., 1999. FE modelling of mining-induced energy release and storage rates. *J. S. Afr. Inst. Min. Metall.* 99 (2), 103–110.
- NB/T 10143-2019, 2019. The Energy Industry Standard of China. Technical Code for Rockburst Risk Assessment of Hydropower Project. China Water and Power Press, Beijing.
- Neyman, B., Szcwoka, Z., Zuberek, W., 1972. Effective methods for fighting rockbursts in Polish collieries. *Proceedings 5th International Strata Control Conference* 23–31.
- Qiu, S.L., Feng, X.T., Zhang, C.Q., Wu, W.P., 2011. Development and validation of rockburst vulnerability index (RVI) in deep hard rock tunnels. *Chin. J. Rock Mech. Eng.* 30 (6), 1126–1141 (in Chinese).
- Singh, S.P., 1988. Burst energy release index. *Rock Mech. Rock Eng.* 21 (2), 149–155.
- Simser, B.P., 2019. Rockburst management in Canadian hard rock mines. *J. Rock Mech. Geotech. Eng.* 11 (5), 132–139.
- Su, Y.Q., Gong, F.Q., Luo, S., Liu, Z.X., 2021. Experimental study on the energy storage and dissipation characteristics of granite under two-dimensional compression with constant confining pressure. *J. Cent. South Univ.* 28 (3), 848–865.
- Szcwoka, Z., Domzal, J., Ozana, P., 1973. Energy Index of Natural Bursting Ability of Coal (In Polish). *Transactions of the Central Mining Institute*, 594.
- Tan, Y.A., 1992. Discussion on the energy impact index of rockburst. *Hydrogeol. Eng. Geol.* 19 (2), 10–12.
- Tang, C.A., Wang, J.M., Zhang, J.J., 2010. Preliminary engineering application of microseismic monitoring technique to rockburst prediction in tunneling of Jinping II project. *J. Rock Mech. Geotech. Eng.* 2 (3), 193–208.
- Tjongkie, T., 1986. Rockbursts, Case Records, Theory and Control. *International Symposium Engineering in Complex Rock Formation*, Beijing, China, pp. 32–47.
- Wang, J.A., Park, H.D., 2001. Comprehensive prediction of rockburst based on analysis of strain energy in rocks. *Tunn. Undergr. Space Technol.* 16 (1), 49–57.
- Wang, Z.L., Yao, J.K., Tian, N.C., Zheng, J.B., Peng, G., 2018. Mechanical behavior and damage evolution for granite subjected to cyclic loading, 2018 *Adv. Mater. Sci. Eng.* 1–10.
- Xie, H.P., Peng, R.D., Ju, Y., Zhou, H.W., 2005. On energy analysis of rock failure. *Chin. J. Rock Mech. Eng.* 24 (15), 2603–2608 (in Chinese).
- Xie, H.P., Li, L.Y., Peng, R.D., Ju, Y., 2009. Energy analysis and criteria for structural failure of rocks. *J. Rock Mech. Geotech. Eng.* 1 (1), 11–20.
- Xu, L., Gong, F.Q., Liu, Z.X., 2021. Experiments on rockburst proneness of pre-heated granite at different temperatures: insights from energy storage, dissipation and surplus. *J. Rock Mech. Geotech. Eng.* <https://doi.org/10.1016/j.jrmge.2021.08.004>.
- Zhang, C.Q., Feng, X.T., Zhou, H., Qiu, S.L., Wu, W.P., 2012. Case histories of four extremely intense rockbursts in deep tunnels. *Rock Mech. Rock Eng.* 45 (3), 275–288.
- Zhang, J.F., Jiang, F.X., Zhu, S.T., Zhang, L., 2016. Width design for gobs and isolated coal pillars based on overall burst-instability prevention in coal mines. *J. Rock Mech. Geotech. Eng.* 8 (4), 551–558.



Fengqiang Gong obtained his BSc and MSc degrees from Central South University (CSU), China, and PhD degree from CSU and Swiss Federal Institute of Technology in Lausanne (EPFL). He is a professor in the School of Civil Engineering at Southeast University (SEU), a part-time professor at Hunan University of Science and Technology, and guest professor at International Joint Research Laboratory of Henan Province for Underground Space Development and Disaster Prevention. His current research interests include failure mechanism of rockburst (coal burst) and spalling, rock energy storage law and application, rock dynamics, strength weakening mechanism of deep rock, and damage constitutive model. He is a member of the International Society for Rock Mechanics and Rock Engineering (ISRM) and International Association for Engineering Geology and the Environment (IAEG), the Vice Chairman of Professional Committee of Rock Breaking Engineering and Deputy Secretary General of Professional Committee of Rock Dynamics of Chinese Society for Rock Mechanics and Engineering (CSRME). He was invited to give a plenary lecture at the 11th “Tjongkie Tan Lecture”—the highest academic forum of rock mechanics and Engineering in China, and also won the “Tjongkie Tan Award” for 2020 outstanding paper in *Chinese Journal of Rock Mechanics and Engineering* in 2021. He was selected as an Elsevier 2020, 2021 Most Cited Chinese Researchers and the world’s top 2% scientists (Single year impact) from 2020 to 2022 by Stanford University. He is a member of the editorial boards of *Chinese Journal of Rock Mechanics and Engineering*, *Journal of Engineering Geology* and *Journal of Mining and Strata Control Engineering*.